Proc. Natl. Acad. Sci. USA
Vol. 82, pp. 948–952, February 1985
Physiological Sciences

Voltage-dependent sodium and potassium channels in mammalian cultured Schwann cells

(single channels)

P. SHRAGER*, S. Y. CHIU, AND J. M. RITCHIE†

Department of Pharmacology, Yale University School of Medicine, New Haven, CT 06510

Communicated by Joseph F. Hoffman, October 10, 1984

ABSTRACT **Cultured Schwann cells from sciatic nerves of newborn rabbits and rats have been examined with patch-clamp techniques. In rabbit cells, single sodium and potassium channels have been detected with single channel conductances of 20 pS and 19 pS, respectively. Single sodium channels have a reversal potential within 15 mV of E_{Na}, are blocked by tetrodotoxin, and have rapid and voltage-independent inactivation kinetics. Single potassium channels show current reversal close to E_K and are blocked by 4-aminopyridine. From these results, and from comparisons of single-channel and whole-cell data, we show that these Schwann cells contain voltage-dependent sodium and potassium channels that are similar in most respects to the corresponding channels in mammalian axonal membranes. Cultured rat Schwann cells also have sodium channels, but at a density about 1/10th that of rabbit cells, a result in agreement with saxitoxin binding experiments on axon-free sectioned nerves. Saxitoxin binding to cultured cells suggests that there are up to 25,000 sodium channels in a single rabbit Schwann cell. We speculate that *in vivo* Schwann cells in myelinated axons might act as a local source for sodium channels at the nodal axolemma.**

Soon after a rat sciatic nerve is cut and allowed to degenerate, the ability of the distal degenerated stump to bind saxitoxin (STX), which has been widely used as a specific marker for the voltage-dependent sodium channels of excitable tissue, virtually completely disappears (1). However, in the rabbit sciatic nerve under the same conditions, the axon-free degenerated stump is found to bind substantial amounts of the toxin (1). This latter binding of STX increases during the several days immediately following sectioning, a time during which Schwann cells proliferate in the distal region and occupy the space vacated by the degenerating axons. Squid Schwann cells (2) and human glial cells (3) are already known to possess sodium channels that are opened by veratridine and blocked by tetrodotoxin (TTX). However, neither these latter experiments (which measured the entry of ^{22}Na into cells) nor the STX experiments provide unequivocal evidence for the presence of voltage-dependent sodium channels of the kind necessary for excitability.

Electrophysiological experiments using the patch-clamp technique have already shown that in rat cultured Schwann cells there are both anion-selective and cation-selective channels (4, 5). The latter, however, are calcium-activated, show no selectivity for sodium compared to potassium, and lack the characteristic voltage dependence of the sodium channels found in excitable tissues. This latter finding is consistent with the earlier finding of a lack of STX binding capacity of the Schwann cells in rat distal degenerated stumps (1). The present experiments show by contrast that rabbit Schwann cells do indeed possess a relatively high density of voltage-dependent sodium channels, in conformity with the findings of the earlier experiments that they bind STX avidly (1). They also possess voltage-dependent potassium channels. We have characterized the electrophysiological properties of these sodium and potassium channels, showing that each is similar in many respects to the corresponding channel in rabbit myelinated axons.

MATERIALS AND METHODS

Preparation of Primary Cultured Schwann Cells. Schwann cells were cultured from the sciatic nerves of newborn rabbits and rats (see ref. 5). The cells were dissociated by a neutral protease (Dispase, 5 mg/ml) and collagenase (1 mg/ml), plated on collagen-coated coverslips, and incubated in Dulbecco's modified Eagle's medium at 37°C. Virtually all experiments were done on cells 3–6 days after plating. Although Schwann cells may sometimes resemble fibroblasts (6), they normally have a characteristic bipolar spindle shape that is quite distinct from the flat multipolar appearance of the contaminating fibroblasts that form the only other cellular component in the culture. Proliferation of these fibroblasts was inhibited in many cultures by adding cytosine arabinoside (15 μM) to the medium. All of the Schwann cells studied electrophysiologically in the present experiments were therefore identified morphologically.

Electrophysiological Recording. Ionic currents were recorded by the patch-clamp technique (7) using both outside-out excised patches and the whole-cell recording configuration. The patch clamp used was the List L/M EPC-5. For whole-cell recording another clamp (the "Yale" clamp) with a lower feedback resistor (1 instead of 10 gigohms) was usually used. The patch pipettes had a resistance of 1–10 megohms and were fire polished. The pipette solutions are indicated in the text according to their predominant salt. Thus, the solution KCl 140 contained (mM) KCl, 140; $CaCl_2$, 1; $MgCl_2$, 2; EGTA, 10; Hepes buffer, 10; the pH of the solution was brought to 7.2 by addition of 29 mM NaOH. The solutions CsCl 140 and CsF 140 were identical to KCl 140 except for substitution of the indicated salt for KCl.

The Locke's solution in the bath contained (mM) NaCl, 154; KCl, 5.6; $CaCl_2$, 2.2; morpholinopropionyl sulfonate (pH 7.4), 10.

Both single-channel currents and whole-cell currents were filtered by an 8-Pole Bessel filter at 1–4 kHz (usually 2 kHz). The preparation was always held initially at a holding potential of −75 mV and then was stepped for 10–100 msec to a new test potential. The electrical responses were sampled at intervals of 50–200 μsec and then stored for subsequent analysis in a DEC 11/34 computer.

The publication costs of this article were defrayed in part by page charge payment. This article must therefore be hereby marked "*advertisement*" in accordance with 18 U.S.C. §1734 solely to indicate this fact.

Abbreviations: STX, saxitoxin; TTX, tetrodotoxin.

*Present address: Department of Physiology, University of Rochester Medical Center, Rochester, NY 14642.
†To whom reprint requests should be addressed.

STX Binding. In some experiments the STX binding capacity (8) of the cultured Schwann cells was determined with [^{3}H]STX (specific activity, 79 dpm/fmol; purity, 85%). Cells from two to four plates were pooled and aliquots were exposed to the [^{3}H]STX for 30 min in the presence and absence of 1 μM TTX. The latter is sufficient to inhibit completely the saturable uptake of [^{3}H]STX and the difference between the two readings gives the saturable uptake. All uptakes were determined in triplicate and the uptake was expressed per mg of protein determined by the Lowry method (9). The experiments were carried out at room temperature (20°C). Wherever possible, mean values ± the standard errors of the means are quoted.

RESULTS

Sodium Channels. Fig. 1*A* shows current records obtained from an "outside-out" patch excised from a rabbit Schwann cell. The patch was held at an initial potential of −75 mV and was stepped to the potentials indicated. The pipette solution in this experiment was CsCl 140, which eliminated potassium currents. As Fig. 1*A* shows, channels that were initially closed at the holding potential opened on depolarization with resulting inward current. With increasing depolarization the amplitude of the single-channel currents decreased.

We examined the dependence of amplitude on test membrane potential by constructing histograms and calculating average values. Fig. 1*B* shows a typical result, in this case at −5 mV, where the mean value was 1.44 pA. These average values were then plotted against voltage (Fig. 1*C*). A straight line fitted to the data by a least squares procedure gave by extrapolation a reversal potential of +57 mV. This is close to the calculated value for the sodium equilibrium potential (E_{Na}) of +42 mV. Furthermore, the inward currents shown in Fig. 1*A* were completely abolished by addition of 100 nM TTX to the bathing medium. These channels are therefore likely to be of the type that contribute to the whole-cell sodium currents recorded previously in rabbit Schwann cells (10). From the slope of the line in Fig. 1*C*, we calculate the single-channel conductance to be 20.0 pS.

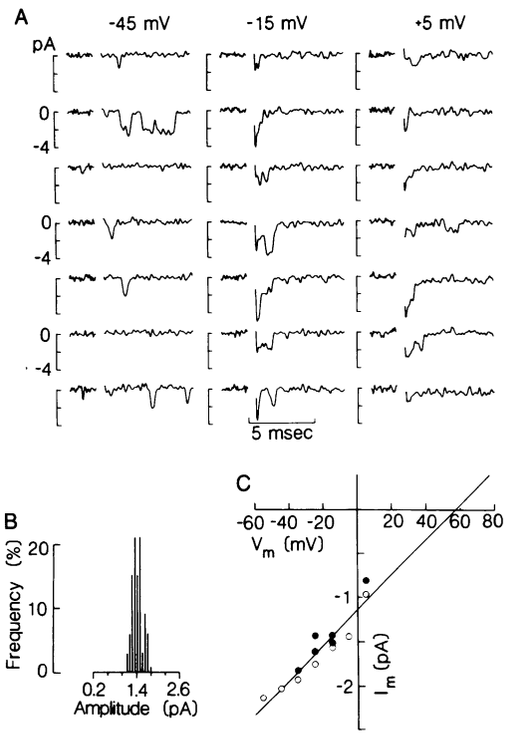

FIG. 1. (*A*) Currents through single sodium channels. The records are from an outside-out patch excised from a rabbit Schwann cell. The patch was held at −75 mV and pulsed to the test potentials indicated at the top of each column. The pipette solution was CsCl 140. Each record contains a baseline segment (sampled at 100-μsec intervals), a blank region (to omit the capacitative transient), and a test segment (sampled at 50-μsec intervals). (*B*) Histogram of single-channel current magnitudes at −5 mV. (*C*) Current–voltage relations for single sodium channels. Current amplitudes represent averages calculated at each voltage as in *B*. The straight line represents a least squares fit to the data.

We have analyzed the single-channel kinetics and compared the results with those obtained from whole-cell records. Fig. 2*A* shows a cumulative open-time histogram (11) for 47 channel openings obtained in 64 consecutive pulses from −75 to −15 mV. The superimposed curve is a single exponential function with a time constant of 305 μsec. When the 64 consecutive traces were summed the time course of the resulting average current for this population of channels was obtained (Fig. 2*B*). At this potential the rising phase could not be resolved. The falling phase, however, is clearly fitted by a single exponential function whose time constant is 746 μsec.

Fig. 1*C* shows the whole-cell sodium currents at −25, −15, and −5 mV. The pipette solution was KCl 140 and the sodium currents were obtained by subtracting sweeps after adding 60 nM TTX to the bath. The falling phases were then fitted by single exponential functions whose time constants were 1.85, 1.24, and 1.04 msec, respectively, and which are superimposed on the records.

Aldrich *et al.* (12) have recently shown in mammalian cultured neuroblastoma and other cells that the time constants obtained from macroscopic whole-cell currents (as in Fig. 2 *B* and *C*) and those obtained from the open-time distribution relationship (as in Fig. 2*A*) differ in two important respects. First, the time constants of decay of the whole-cell currents (conventionally interpreted as "inactivation") are greater than the time constants obtained from the open-time histogram. Second, though the time constants of the whole-cell currents are markedly voltage-dependent, those obtained from the open-time histogram are not. In Fig. 3 we show that a similar phenomenon is seen in Schwann cells. The time constants of the falling phases of the currents in whole-cell records (plotted as solid symbols) clearly differ from those obtained from open-time histograms (plotted as open symbols) in the same way as described for the other mammalian cells studied by Aldrich *et al.* (12).

It is of interest that the time constants obtained from summing the single-channel records (× and +, Fig. 2*B*) are of the same order of size as the time constants obtained from whole-cell recordings. This suggests that there are no major series resistance errors of recording and that in the whole-cell records the channels that contribute to these currents are largely in the "cell body" as opposed to the long bipolar processes.

Fig. 2*D* shows, for comparison, the corresponding whole-cell records in rat Schwann cells, which are considerably smaller than in rabbit cells (see also below).

An important issue is whether the sodium channels in rabbit Schwann cells resemble those in rabbit nodes. Fig. 4 compares the voltage dependence of sodium inactivation (*h*-infinity) and of sodium activation (peak current–voltage) relations in rabbit nodes and rabbit Schwann cells. The open symbols show data obtained from whole-cell currents in three Schwann cells; the peak current–voltage data in these experiments have been normalized so that the maximal peak inward current in each trace is unity. The solid symbols show the *h*-infinity relationship in these same cells. Superimposed on Fig. 4 are the corresponding relations (solid lines) obtained by Chiu *et al.* (13) for the axolemmal sodium channels in the node of Ranvier in the same species. In the latter case, the position of the *h*-infinity curve on the voltage axis

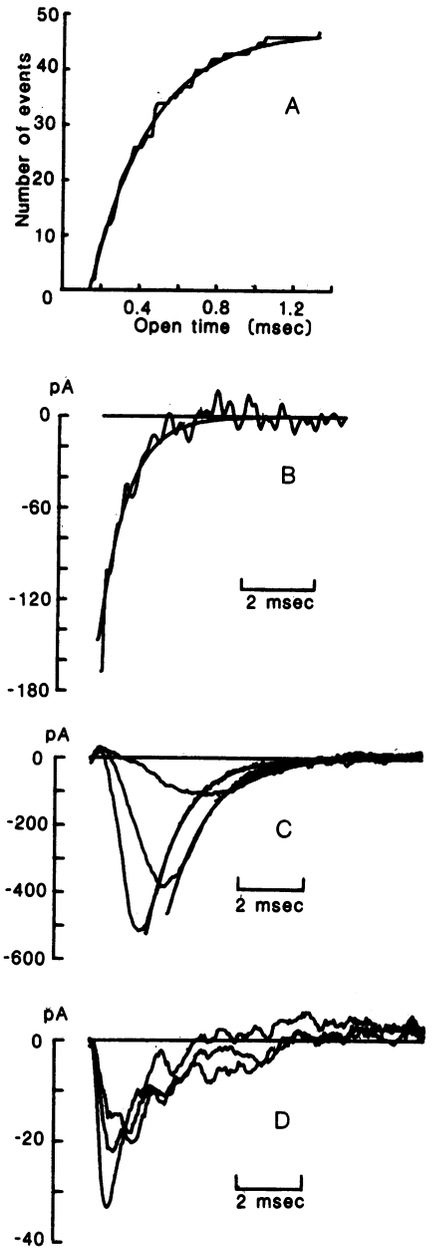

FIG. 2. Sodium channel kinetics from single-channel and whole-cell records. (*A*) Cumulative open-time histogram for single sodium channels. The number of open times less than or equal to a given time t is plotted against t. The histogram included 47 events at a test membrane potential of −15 mV. The superimposed single exponential fit has a time constant of 305 μsec. (*B*) Summed single sodium channel records. The same 64 consecutive sweeps used in *A* were summed. At this potential the rising phase was not resolved. The falling phase has been fitted by a single exponential function of time constant 746 μsec. (*C*) Whole-cell sodium currents at −25, −15, and −5 mV. The pipette solution was KCl 140. Sodium currents were obtained by subtracting sweeps after adding 60 nM TTX to the bath. The falling phases were fitted by the superimposed single exponential functions of time constants 1.85, 1.24, and 1.04 msec, respectively. (*D*) As in Fig. 2*C* for rat instead of rabbit Schwann cells.

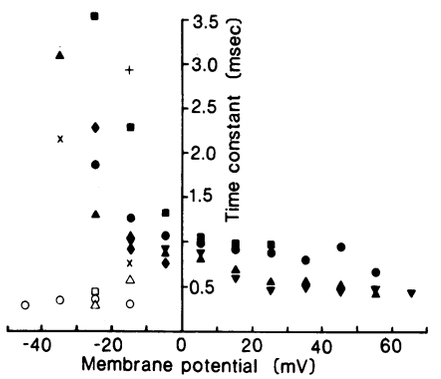

FIG. 3. Time constants as a function of membrane potential. The solid symbols show the falling phase time constants from whole-cell records (as in Fig. 2*C*). The symbols × and + are from sums of single-channel records (as in Fig. 2*B*). The open symbols represent data from open-time histograms as in Fig. 2*A*.

is set by assigning a value of −75 mV to the potential at which the value of h-infinity is 0.75 (see ref. 13). It should be noted that the extrapolated reversal potential for the Schwann cell sodium current in the peak current–voltage plot (Fig. 4) is well above the expected E_{Na} of 30–50 mV. Indeed, in most experiments the sodium currents did not reverse even at large depolarizations. A likely explanation is that the long spindle shape of the Schwann cell with its long processes (up to 200 μm in length) at either end introduces spatial nonuniformities in the voltage control. As the cell body is depolarized to E_{Na} distant channels will be activated. These distant channels, however, see a much attenuated voltage, presumably because of the high cytoplasmic resistance of the narrow spindle and its processes. The currents they produce would thus be inward, which would mask the reversal of the currents at the cell body proper. Despite this, Fig. 4 permits two important comparisons between the sodium channels of Schwann cells and axons to be made. First, if the two cells are held at potentials producing the same degree of steady-state inactivation, Schwann cells require a significantly stronger depolarization than do axons to activate sodium channels. Second, the slopes of the h-infinity curves and of the negative conductance regions of the peak current–voltage curves are similar in the two cells.

Potassium Channels. Fig. 5*A* shows the results of experiments on the currents through single potassium channels. The records are from an outside-out excised patch and were obtained with KCl 140 in the pipette. These single channel currents were blocked by 4-aminopyridine (6 mM) added to the bath and required the presence of potassium ions in the

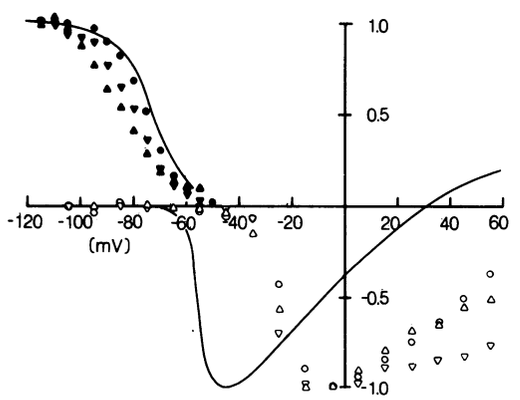

FIG. 4. Comparison of sodium channels in rabbit Schwann cells and in rabbit node of Ranvier. The solid symbols represent steady-state inactivation (h-infinity) and the open symbols give the peak current–voltage relation (normalized to a common maximal peak inward current) for several rabbit cultured Schwann cells. The h-infinity relations were obtained by normalizing the peak sodium currents elicited by a test pulse to −5 mV preceded by a 100- to 200-msec prepulse to the indicated voltages. The pipette solutions were either KCl 140 or Cs 140. The external solution was Locke's. The lines are the corresponding h-infinity and current–voltage relations taken from Chiu *et al.* (13) for rabbit nodal sodium channels.

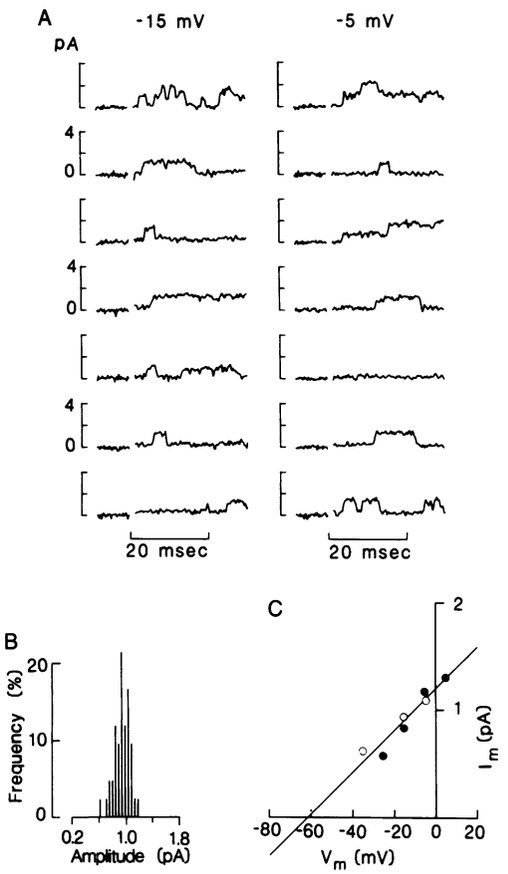

FIG. 5. Current–voltage relations for single potassium channels. (*A*) Currents through single potassium channels. Records are from an outside-out excised patch. The pipette solution was KCl 140. Baselines were sampled at 400-μsec intervals and test pulses were sampled at 200 μsec per point. (*B*) Histogram of amplitudes of single channel potassium currents at −15 mV. (*C*) Current–voltage relations for single potassium channels. The average single channel current for 42 channels (obtained as in *B*) is plotted against membrane potential. The straight line represents the least squares fit to the experimental points.

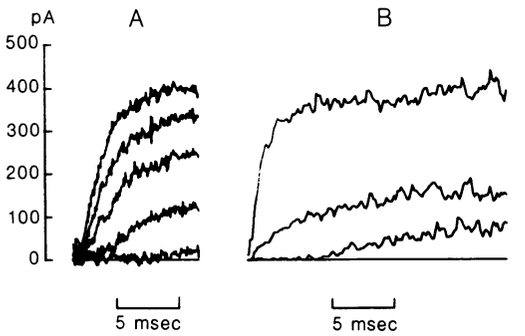

FIG. 6. Voltage dependence of potassium currents. (*A*) Potassium currents recorded by using the whole-cell technique at test potentials of −35 to +5 mV (in 10-mV steps). The pipette solution was KCl 140 and the bath included 60 nM TTX. (*B*) Potassium currents derived from single-channel records. At each test potential (−15, −5, and +5 mV), 64 successive sweeps were analyzed and simulated records were summed. The trace at +5 mV was scaled to match the corresponding trace in *A*. The pipette and bath solutions were as in *A*.

pipette solution. Fig. 5 *B* and *C* show the same kind of analysis for potassium channels as was carried out in Fig. 1*A* for sodium channels. From the amplitude histograms (Fig. 5*B*) at a variety of membrane potentials (Fig. 5*C*) one obtains a single-channel conductance of 19 pS and an extrapolated reversal potential of −63 mV, which is to be compared with a theoretical value for the potassium equilibrium potential E_K of −77 mV. For these reasons, these channels were identified as the potassium channels that are responsible for the delayed rectifier potassium currents seen in whole-cell records (10). Fig. 6*A* shows whole-cell potassium currents recorded from a rabbit Schwann cell after adding 60 nM TTX to the bath to block completely any sodium currents. In Fig. 6*B* idealized single-channel traces were simulated (as in figure 13-1 of ref. 14) and then summed. The summed currents were scaled by a constant factor so that the steady-state value at +5 mV was equal to that of the corresponding whole-cell current. The kinetic behavior of the summed single-channel currents is similar to that of the whole-cell traces, and their voltage dependence differs by <15 mV.

Sodium and Potassium Channels in Rat Schwann Cells. Rat Schwann cells were examined with the whole-cell patch configuration. An example of sodium currents recorded in this manner is given in Fig. 2*D*. As in the rabbit Schwann cells these currents were blocked by externally applied TTX. The maximal peak inward currents recorded from rat cells were consistently much smaller than in rabbit Schwann cells. Of 11 rat Schwann cells studied, 6 had no measureable sodium current (the limit of detection being about 5 pA), whereas the remaining 5 cells had peak inward currents of 18–68 pA (mean, 36.7 ± 9.2 pA). By contrast, the corresponding maximal peak sodium current in rabbit Schwann cells ranged from 50 to 2100 pA and had a mean value of about 500 pA (10). If the pipette solution was KCl 140, potassium currents could also be found in rat cells. These have not been studied in detail. The steady-state potassium current was typically about 100 pA at +65 mV, but in 1 cell it was 1400 pA.

[^{3}H]STX Binding to Schwann Cells. Rat cultured Schwann cells, unlike those *in vivo* (1), do seem to bind [^{3}H]STX, but they do so to a much smaller extent than do rabbit cultured Schwann cells. Thus, when tested at a concentration of about 5 nM—i.e., at about 2½ times the equilibrium dissociation constant (K) of about 2 nM for STX (unpublished data) in this preparation—rabbit Schwann cells bound about 128 ± 13 (n = 22) fmol/mg of protein; the corresponding rat cells bound only 13 ± 3 (n = 5) fmol/mg of protein. Based on a value for K of 2 nM, the maximal uptake by the rabbit Schwann cell would be about 180 fmol/mg of protein.

DISCUSSION

Density of Sodium Channels on Rabbit Schwann Cells. Our present experiments clearly show that the plasma membrane of rabbit Schwann cells is rich in voltage-sensitive sodium channels, thus confirming the earlier observations that these cells avidly bind STX (1). In photomicrographs (10) rabbit cultured Schwann cells appear as bipolar cells about 50 μm long and 10 μm in diameter at the center. Assuming that the two halves of the cell (excluding the long processes at either end) are cones, one calculates a surface area for the cell body of about 800 μm^2 and a volume of about 1300 μm^3. If the protein composition of the Schwann cell resembles that of a typical mammalian cell, being about 18% of its wet weight (see table 3-1 of ref. 15), the maximal [^{3}H]STX binding calculated above of 180 fmol/mg of protein corresponds to an uptake of 32 fmol/mg of wet weight of Schwann cell. It is interesting that this value, though not equal to, is of the same order of size as the binding of about 40 fmol/mg of wet weight obtained for *in vivo* preparations of Schwann cells in degenerated distal stumps (1). Based on the present findings, therefore, the cultured Schwann cells appear to bind about 25,000 STX molecules per cell, which, if confined to the

plasmalemma of the cell body, corresponds to a site density of 30 per μm^2.

By contrast, the patch-clamp experiments suggest a much smaller value. From a cell that gave the biggest sodium currents, we calculated the maximal sodium conductance from the peak sodium currents. The sodium conductance asymptotes to a value of about 18.4×10^{-9} S between +15 and +75 mV. With a single-channel conductance of 20 pS this corresponds to 920 channels for the cell or a density of only about 1 site per μm^2.

Kinetics of Sodium Channel Activation and Inactivation. Our results on Schwann cells agree with the findings of Aldrich *et al.* (12) obtained on other mammalian cells. Time constants of decay of whole cell currents are highly voltage-dependent and are much larger than inactivation time constants calculated from open-time histograms. The latter are virtually independent of potential over the range studied.

Function of Schwann Cell Sodium and Potassium Channels. Voltage-dependent potassium channels have been described previously for nonneuronal tissue (16). However, voltage-dependent sodium channels are much more restricted in their distribution, and they have, until now, only been found in neuronal and muscle excitable tissue. Although squid Schwann cells (2), human glial cells (3), as well as human and hamster fibroblasts (3, 17) have been shown to possess sodium channels that are opened by veratridine and blocked by TTX, no voltage-dependence has been demonstrated under voltage-clamp conditions. The present experiments now show that rabbit Schwann cells have all of the machinery of electrical excitability. Nevertheless, it is unlikely the Schwann cell sodium channels subserve any role of conduction, if only because the normal resting potential of the cultured Schwann cells is about −40 mV (10), a potential at which all sodium channels would be inactivated. One possible explanation for their presence is that the Schwann cells provide a local source of sodium (and perhaps potassium) channels for the axolemma of the neurons they ensheath. This would provide for a replenishment of the axolemmal channels during their normal life cycle, which would complement their replenishment by axonal transport from a distant neuronal cell body. It is pertinent to mention in this connection that transfer of molecules even as large as proteins from Schwann cells and glial cells to axons (and in the reverse direction) is now well established (see, for example, ref. 18). Furthermore, the Schwann cells at peripheral nodes of Ranvier direct a dense network of microvilli radially inward to end as a regularly spaced hexagonal array in close relationship to the nodal axolemma (19). These observations thus provide both a biochemical and morphological basis for the Schwann cells acting as local factories for axolemmal channels. This speculation might account for the puzzling observation, both in STX binding experiments (1) and in the present electrophysiological experiments, that the density of sodium channels on rat Schwann cells is at least an order of magnitude smaller than in the rabbit. Certain nervous parameters do not scale as the size of the species varies. In particular, although the length of corresponding segments of the sciatic nerve may be 10 times larger in the rabbit than the rat, the spectrum of fiber diameters is more-or-less the same in the two species. The problem of transport of sodium channels from the cell body to a distant node would therefore be much less severe in the rat than in the rabbit, which might account for there being less need for a local channel factory. A similar argument would account for the absence of STX binding to the glia of the two central nervous system preparations studied so far, the glial cells of optic nerves of *Necturus* (20) and of the rabbit (21). In both of these preparations the distances between the cell bodies and all parts of their axons are relatively short.

Whether or not this highly speculative suggestion obtains, the fact remains that the rabbit cultured Schwann cell possesses both voltage-dependent sodium and potassium channels for which no other function more directly appropriate suggests itself.

We thank Drs. Richard Aldrich and David Corey for invaluable help with patch-clamp techniques. Ms. Bhagya Subramanian provided expert technical assistance in cell culturing. This work has been supported by Grants NS08304, NS12327, and NS17965 from the Public Health Service and by Grant RG 1162 from the U.S. National Multiple Sclerosis Society.

1. Ritchie, J. M. & Rang, H. P. (1983) *Proc. Natl. Acad. Sci. USA* **80,** 2803–2807.
2. Villegas, J., Sevcik, C., Barnola, F. V. & Villegas, R. (1976) *J. Gen. Physiol.* **67,** 369–380.
3. Munson, R., Westermark, B. & Glaser, L. (1979) *Proc. Natl. Acad. Sci. USA* **76,** 6425–6429.
4. Bevan, S., Gray, P. T. A., Rang, H. P. & Ritchie, J. M. (1984) *J. Physiol. (London)* **348,** 17P.
5. Gray, P. T. A., Bevan, S. & Ritchie, J. M. (1984) *Proc. R. Soc. London Ser. B* **221,** 395–409.
6. Brockes, J. P., Fryxell, K. J. & Lemke, G. E. (1981) *J. Exp. Biol.* **95,** 215–230.
7. Hamill, O. P., Marty, A., Neher, E., Sakmann, B. & Sigworth, F. J. (1981) *Eur. J. Physiol.* **391,** 85–100.
8. Ritchie, J. M. & Rogart, R. B. (1977) *Rev. Physiol. Biochem. Pharmacol.* **79,** 1–50.
9. Lowry, O. H., Rosebrough, N. J., Farr, A. L. & Randall, R. J. (1951) *J. Biol. Chem.* **193,** 265–275.
10. Chiu, S. Y., Shrager, P. & Ritchie, J. M. (1984) *Nature (London)* **311,** 156–157.
11. Colquhoun, D. & Hawkes, A. G. (1983) in *Single-Channel Recording*, eds. Sakmann, B. & Neher, E. (Plenum, New York), pp. 135–175.
12. Aldrich, R. W., Corey, D. P. & Stevens, C. F. (1983) *Nature (London)* **306,** 436–441.
13. Chiu, S. Y., Ritchie, J. M., Rogart, R. B. & Stagg, D. (1979) *J. Physiol. (London)* **292,** 149–166.
14. Aldrich, R. W. & Yellen, G. (1983) in *Single-Channel Recording*, eds. Sakmann, B. & Neher, E. (Plenum, New York), pp. 287–299.
15. Alberts, B., Bray, D., Lewis, J., Raff, M., Roberts, K. & Watson, J. D. (1983) *Molecular Biology of the Cell* (Garland, New York), p. 92.
16. DeCoursey, T. E., Chandy, K. G., Gupta, S. & Cahalan, M. D. (1984) *Nature (London)* **307,** 465–468.
17. Pouyssegur, J., Jacques, Y. & Lazdunski, M. (1980) *Nature (London)* **286,** 162–164.
18. Kriegler, J. S., Krishnan, N. & Singer, M. (1981) *Adv. Neurol.* **31,** 479–504.
19. Landon, D. & Hall, S. (1976) in *The Peripheral Nerve*, ed. Landon, D. (Wiley, New York), pp. 1–105.
20. Tang, C. M., Strichartz, G. R. & Orkand, R. K. (1979) *J. Gen. Physiol.* **74,** 629–642.
21. Pellegrino, R. G. & Ritchie, J. M. (1984) *Proc. R. Soc. London Ser. B.* **222,** 155–160.